


Cyanidium chilense (Cyanidiophyceae, Rhodophyta) from tuff rocks of the archeological site of Cuma, Italy

Claudia Ciniglia¹ ^{*}, Paola Cennamo,² Antonino De Natale,³ Mario De Stefano,¹ Maria Sirakov,¹ Manuela Iovinella,⁴ Hwan S. Yoon⁵ and Antonino Pollio³

¹Department of Environmental, Biological and Pharmaceutical Science and Technology, University of Campania “L. Vanvitelli”, Caserta, Italy, ²Department of Biology, Facoltà di Lettere, Università degli Studi ‘Suor Orsola Benincasa’, Naples, Italy, ³Department of Biology, University of Naples Federico II, Naples, Italy, ⁴Department of Biology, University of York, York, UK and ⁵Department of Biological Sciences, Sungkyunkwan University, Seoul, South Korea

SUMMARY

Phlegrean Fields is a large volcanic area situated southwest of Naples (Italy), including both cave and thermoacidic habitats. These extreme environments host the genus *Cyanidium*; the species *C. chilense* represents a common phototrophic microorganism living in anthropogenic caves. With a view to provide a comprehensive characterization for a correct taxonomic classification, morpho-ultrastructural investigations of *C. chilense* from Sybil’s cave (Phlegren Fields) was herein carried out and compared with the thermoacidophilic *C. caldarium*. The biofilm was also analyzed to define the role of *C. chilense* in the establishment of a biofilm within cave environments. Despite the peculiar ecological and molecular divergences, *C. chilense* and *C. caldarium* shared all the main diacritic features, suggesting morphological convergence within the genus; cytological identity was found among *C. chilense* strains geographically distant and adapted to different substrates, such as the porous yellow tuff of Sybil cave, and calcyte, magnesite and basaltic rocks from other caves. *C. chilense* is generally dominant in all biofilms, developing monospecific islets, developing both superficially or between fungal hyphae and coccoid cyanobacteria. Extracellular polymeric substances (EPS) were recorded in *C. chilense* biofilms from Sybil cave, confirming the role of EPS in facilitating cells adhesion to the surface, creating a cohesive network of interconnecting biofilm cells.

Key words: biofilm, cave, *Cyanidium caldarium*, extremophile.

INTRODUCTION

Brock (1978) defined extreme environments with selective conditions in which only a few organisms, such as prokaryotic and eukaryotic algae, are able to grow and reproduce. In these habitats, algae can live close to the limits of their physiological potential, adapting their life processes at extreme conditions. The main environmental factors limiting the growth of entire groups of organisms are water availability, light intensity, temperature, salinity, acidity, hydrostatic pressure, electromagnetic and ionizing radiation.

The genus *Cyanidium* includes two species, both having a key role in the composition of biofilms occurring in extreme environments: *C. caldarium* (Tilden) Geitler is a polyextremophilic taxon adapted to acidic (pH 0.5–3.0) and

thermal (35–55°C) soils, retrieved from hot springs and fumaroles, worldwide (Ciniglia *et al.* 2014; Eren *et al.* 2018; Iovinella *et al.* 2018); *C. chilense*, formerly ‘cave *Cyanidium*’ (Hoffmann 1994), is a neutrophilic (pH around 7.0) and mesophilic (20–25°C) strain isolated by several authors from caves, considered as extreme environments, since nutrient input, light intensity, temperature, and humidity are limiting factors for microorganisms (Pedersen 2000).

C. chilense was first discovered in five caves in Chile by Schwabe (1936) and reported by the author as *C. chilense*. Since this and other studies of Schwabe in Chile (1936, 1942), *C. chilense* was found in many other sites worldwide: occurring in built and natural stones in Central and South America (Gaylarde *et al.* 2006, 2012), Negev desert in Israel (Friedmann 1964), Tunisia (Darienکو & Hoffmann 2010), France, Spain and Italy (Skuja 1970; Leclerc *et al.* 1983; Cennamo *et al.* 2012; Del Rosal *et al.* 2015). In 2009, Azúa Bustos *et al.* described another population of *C. chilense* from a new site in Chile, the coastal caves of the hyperarid Atacama desert, reporting in detail morphological, ultrastructural and molecular data (Azúa-Bustos *et al.* 2009).

C. chilense colonizes the tuff cave walls of Sybil’s cave (Friedmann 1964; Di Girolamo *et al.* 1984; Cennamo *et al.* 2012, 2016), by layering on the top or inside of the rock cavities, challenging ecological extremes such as lack of water, temperature and humidity fluctuations, excess or depletion of light energy, and the influence of various types of radiation. Unlike *C. caldarium*, which colonizes exclusively volcanic substrates of thermal springs and fumaroles, *C. chilense* is able to adhere also to different rocky surfaces, such as the coastal basaltic caves in the Atacama desert (Azúa-Bustos *et al.* 2009), or the calcite and magnesite crystals of the Spanish touristic caves (Del Rosal *et al.* 2015).

The nomenclature of this meso-neutrophilic *Cyanidium* has changed during the years; Schwabe himself (1942) renamed it as *C. caldarium* var. *chilensis*, due to its close morphological similarity to the thermo-acidophilic *C. caldarium*. The phylogenetic relations between *C. chilense* and *C. caldarium* were first highlighted by using two Italian strains of *C. chilense*, isolated from the anthropogenic tuff

**To whom correspondence should be addressed.*

Email: claudia.ciniglia@unicampania.it

Communicating Editor: Mitsunobu Kamiya

Received 26 November 2018; accepted 6 April 2019.

cave walls of Sybil cave (Phlegren Fields, Italy) and from Monte Rotaro (Phlegrean Fields, Ischia, Italy); molecular analyses based on concatenated three-genes trees confirmed that *C. caldarium* and *Cyanidium* from caves represent two sister-related lineages (Ciniglia *et al.* 2004), thus supporting the nomenclatural reinstatement and recognizing *C. chilense* as a legitimate name for all cave *Cyanidium* isolates (Ciniglia *et al.* 2018). *C. chilense* from the Atacama desert (Chile) was successively shown to belong to the same lineage of the Italian strains (Azúa-Bustos *et al.* 2009), suggesting that a unique *C. chilense* could be distributed worldwide. Successively, a more robust phylogenetic analysis based on six plastid genes supported the monophyly of the mesophilic *Cyanidium* strains and the existence of a different monophyletic super-clade where *C. caldarium* clustered with *G. maxima* and *C. merolae* (Yoon *et al.* 2006); this would suggest a further nomenclatural reinstatement in *Cyanidium* and the institution of a new mesophilic genus within Cyanidiophyceae, thus reclaiming an exhaustive description of the mesophilic taxa not only by molecular but even by morphological and ecological tools. The present study aims at carrying out an ultrastructural characterization of the *C. chilense* strains isolated from tuff wall of the Sybil's cave, in order to assess the morphological similarities/differences with *C. chilense* from Atacama desert and from the touristic Spanish caves (Del Rosal *et al.* 2015), already described in the literature, and with the thermoacidophilic *C. caldarium*.

We also analyzed the biological community of the biofilm and the structure, with the aid of confocal laser scanner microscope (CLSM) and molecular tools (Denaturing Gradient Gel Electrophoresis, DGGE). All results were compared to the data so far available on ecological and morphological features of *C. chilense* biofilms, in order to define the role of *C. chilense* in the establishment of a biofilm within cave environments and to characterize this mesophilic strain.

MATERIAL AND METHODS

Sampling in the archeological site of Cuma

Sybil's cave, located at the Acropolis of Cuma at Phlegrean Fields (UTM: VF12, latitude: 40.847716 longitude: 14.053707. Figure 1a,b) was built in the fourth century BCE. It is a trapezoidal passage over 131 m long running parallel to the side of the hill upon which was built the Acropolis of Cuma at Phlegrean Fields. It was cut out in the volcanoclastic Neapolitan Yellow Tuff. The tuff wall preceding the gallery (Fig. 1c) is exposed to light and to a continuous flux of air, that allowed the development of a green biofilm that extends along the entire surface. On this tuff wall, samples were collected within a square surface (40 × 40 cm) characterized by a light green biofilm, which suggested the abundant presence of *C. chilense*. Five different samples were collected (Fig. 1c I–V), on which scanning electron microscopy (SEM), transmission electron microscopy (TEM), confocal laser scanning microscopy (CLSM) and denaturing gradient gel electrophoresis (DGGE) analyses were performed. Sampling was carried out with sterile scalpels, and the materials were deposited into sterile vials and brought into the laboratory for analyses.

C. chilense colonies were distinguishable since they appeared as a bright green patina, while Cyanobacteria appear dark or light green. Temperature, relative humidity, and light intensity were measured at each sampling site by using appropriate instruments (TESTO 174H 2, TESTO 545, Mitchell Instrument Co., Vista, CA, USA). Light irradiance at each sampling point was measured by using a LI-COR radiation sensor (LI-COR Biosciences, NE, USA).

In order to check the mineral composition of the substrate, the samples were fixed on a graphite stub and quantitative analysis was performed with an X-ray diffractometer (SEM -ZAFPB).

Electron microscopy

C. chilense and *C. caldarium* (ACUF182, www.acuf.net) cells were harvested by centrifugation (2000 *g* for 5 min) and then fixed with 4% formaldehyde buffered with 0.2 M Na-cacodylate (pH 7.5, ratio 1:1) for 1 h at room temperature. The samples were washed three times with 0.1 M Na-cacodylate (pH 6.3), concentrated by centrifugation (2000 *g* for 15 min), and after a final wash in DDW, the pellet was filtered on a 'Nucleopore' polycarbonate filter (Costar, Corning Inc. Lowell, MA, USA) in a Swinnex filtration apparatus (Millipore Ltd., Milan, Italy). A second Nucleopore filter was placed over the first to form a sandwich in which the sample was trapped. The dehydration and the critical point drying procedure were respectively carried out by directly immersing the Swinnex into specific containers in alcohol at increasing ethanol concentration (50%, 60%, 80%, 90%, 95%, 100%) and finally the sample was placed in a critical point dryer (Emitech K575X, Quorum Technologies Ltd., East Grinstead, West Sussex, United Kingdom). At the end of the treatment, the Swinnex was opened and both the filters were placed on Aluminum stubs and sputter-coated with gold. SEM observations were performed at an accelerating voltage of 20 kV using a Jeol 6060Lv Scanning electron microscope (JEOL Ltd. Tokyo, Japan).

TEM observations were performed on a pellet of algal cells of both species fixed with glutaraldehyde 0.1–0.5% at pH 7 (diluted with DDW) and post-fixed with some drops of osmium tetroxide (1% in DDW) after 10–20 min. The pellet was left in OsO₄ for about 5–10 min up to become intensely black-colored then was washed in DDW and dehydrated in ethanol at an increasing concentration (40, 60, 80, and 100%). Dried samples were pre-included in a mixture of propylene oxide-epoxide resin at increasing strength (30, 60%) and then included in epoxide resin (with several exchanges of 15 min each). After the resin polymerization, the samples were sectioned and the slides stained with uranyl acetate 2% (in 30% methanol for 45 min) and lead citrate. TEM observations were performed at an accelerating voltage of 120 kV using a Leo 912 Omega electron microscope (Carl Zeiss, Oberkochen, Germany).

Scanning electron and laser confocal microscopy on *C. chilense*-biofilms

The microbial populations sampled on the substrate were also analyzed with a Leica TCS SP5 confocal laser scanning microscope (CLSM) by capturing images at HCX PL APO 63.0 × 1.40 oil UV. Sections approximately 1 × 1 cm were cut from adhesive tape samples (Urzi & De Leo 2001).

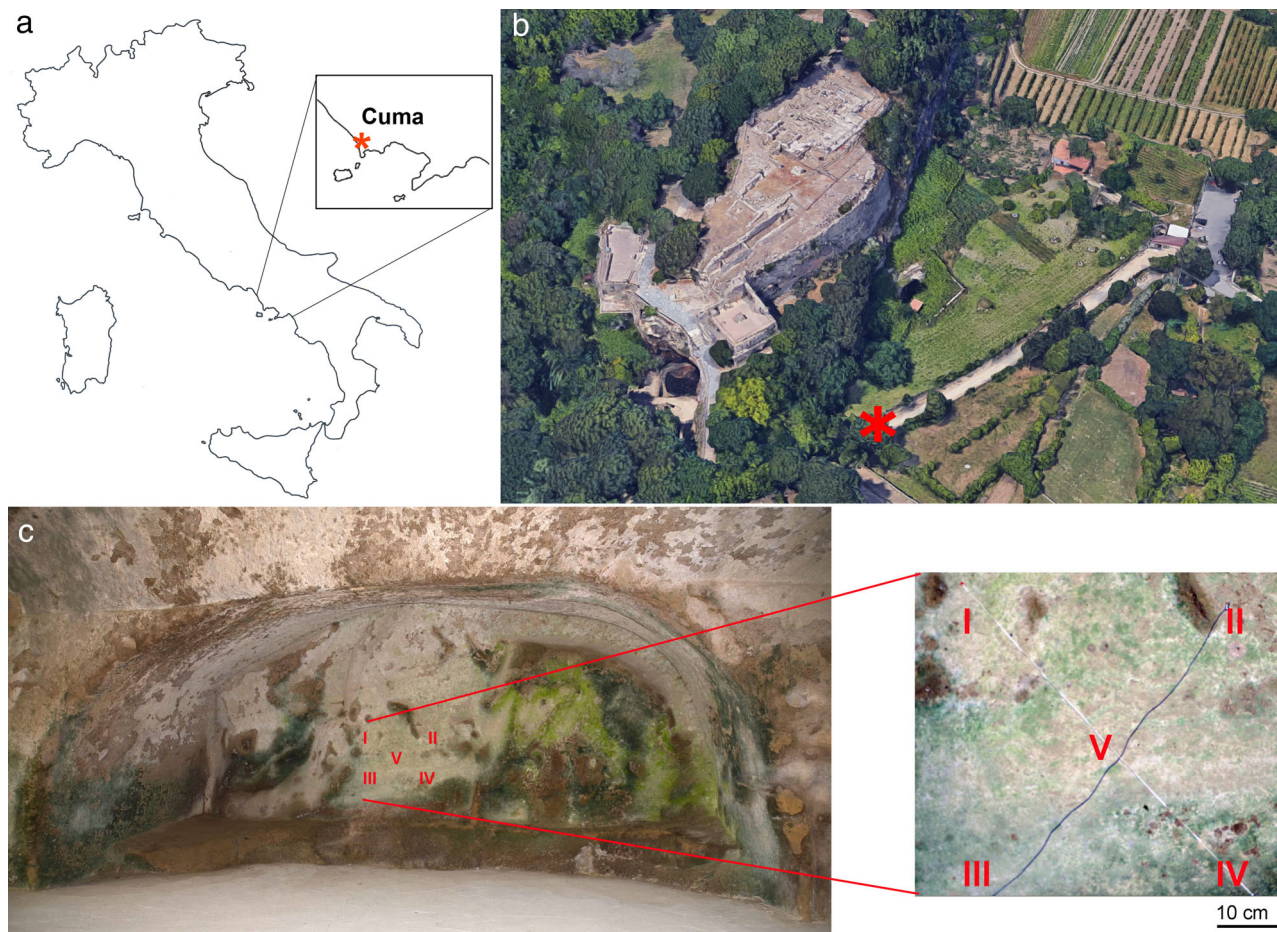


Fig. 1. The sampling site: a small cave neighboring Sybil's cave entrance, Archeological Park of Cuma, Naples (a, b 'Source: <https://www.google.com/maps/search/cuma+scavi/@40.8480199,14.0525435,287m/data=!3m1!1e3>'), and a detail of the five sampling points (I–V) (c).

Measurements were taken from three areas on each section of strips. The images from stacks were captured at 0.50 μm intervals. The substratum area of the image stack was 1024 \times 1024 pixel. The number of images in each stack varied according to the thickness of the biofilm. Images were acquired in the three channels simultaneously: red channel for pigment autofluorescence (chlorophyll-*a* and phycobilins; Carfagna *et al.*, 2018), with excitation beams at 633 nm and emission at 641–737 nm (red channel). The acid polysaccharides of the extrapolymeric matrix (EPS) using the concavalina-A with the Alexa 488, at an excitation beam at 543 nm and emission at 553–637 nm (green channel). The calcofluor-white stain was used to label the bacteria and hyphae with an excitation beam at 405 nm and emission at 415–506 nm (blu channel).

The open source image processing package Fiji (Schindelin *et al.* 2012; and also <http://www.fiji.sc>) was used to evaluate the area of all stacked CLSM images, and to obtain 2D MIPs. The images have been previously converted to 8-bit and then resampled by using the tool Threshold (Bavey 2002; Lepanto *et al.* 2014; Del Mondo *et al.* 2018). Analyze Particles tool was used to determine the areas and perimeters of each slice belonging to Z-stacks (Hartig 2013; Marasco *et al.* 2016). Comstat2 (Heydorn *et al.* 2000) tool was used to determine the volume, thickness, roughness of

each Z-stacks (Hartig 2013). According to Solé *et al.* (2009) for the individual of biomass determination of *C. chilense*, the structures were screened in each original stack. In each z-stack, a structure was initially selected and then erased from the stack. Finally, the Comstat2 plugin was applied to each stack in order to obtain the biomass for *C. chilense* structure in an individual manner, as we calculated in the total of biomass. The cyanobacteria were identified using different morphological criteria according to Castenholz (2001), that is, diameter (μm), cell division patterns, and the presence or absence of a sheath for unicellular morphotypes.

Identification of microbial components of *C. chilense* biofilms

DNA of the environmental samples were extracted using a procedure described by Doyle and Doyle (1990). PCR amplification was carried out on an estimated 10 ng of extracted DNA. For cyanobacteria, primers for 16S rDNA, and for algae, primers for 18S rDNA, were used following the protocol of Cennamo *et al.* (2015) and Ciniglia *et al.* (2015). PCR reactions were carried out in a final volume of 50 μL , containing 5 μL of 10 \times PCR buffer, 100 mM of deoxynucleotide triphosphate, 2.5 mM of magnesium chloride, 0.5 mM of primers, and 1U of Taq polymerase (Quiagen, Hilden, Germany). The

PCR program consisted of an initial denaturation at 95°C for 4 min and 30 cycles including 1 min of denaturation at 94°C, 45 s of annealing at 56°C, and 2 min extension at 72°C. A final extension of 7 min at 72°C followed by cooling at 4°C terminated the PCR program. Aliquots of purified PCR product were ligated into the pGEM-T easy Vector system (Promega, Vienna, Austria), following the manufacturer's instructions. Clones were screened on DGGE (see below) and sequenced with a 3130 genetic analyser (Applied Biosystems, Foster City, CA, USA). The sequences obtained from DGGE bands were aligned to the already available sequences in the database (GenBank). Only the sequences matching at least 90% with literature sequences were considered.

DNA extracted was analyzed by DGGE following the protocol of Diez *et al.* (2001) and Cennamo *et al.* (2015). Electrophoresis was carried out on 0.75 mm thick 6% polyacrylamide gels (acrylamide/bisacrylamide, 37/1) submerged in 1× TAE buffer (40 mM Tris, 40 mM acetic acid, 1 mM EDTA, pH 7) at 60°C. Sixty nanograms of PCR product from environmental samples were applied to individual lanes in the gel. Electrophoresis conditions were 16 h at 100 V. Gels were stained for 30 min in 1 × TAE buffer with SybrGold nucleic acid stain and visualized with UV radiation by using a Fluor-S Multilmager and MultiAnalyst imaging software (BioRad). DGGE bands were sequenced after excision from gel and re-amplification. Briefly, bands were excised, re-suspended in 20 ml of DNase free water and stored at 4°C overnight. The majority of DGGE bands were cloned, sequenced and matched with the GenBank database using the BLASTN algorithm available at the National Center for Biotechnology (NCBI, <https://www.ncbi.nlm.nih.gov>). DGGE analysis was repeated for the artificial biofilm before and after the exposures to EMR.

RESULTS

Sampling site physical parameters

The biofilms analyzed in this study were collected from a cave at the entrance, on the left side before reaching the *dromos* leading to Sybil's cave (Fig. 1c), characterized by the following chemical–physical parameters: relative humidity, light intensity and average temperature recorded in the sampling area were $59 \pm 1\%$, $0.25 \pm 0.001 \mu\text{mol m}^{-2} \text{s}^{-1}$, and $18^\circ\text{C} \pm 2$, respectively. Figure 2 reports the elemental composition of the rock substrates (O, Ca, C, S, N, Si, Mg, Cl, K, Al, Na, Fe, P) which was attributable to the mineralogical composition of the Neapolitan yellow tuff (Cennamo *et al.* 2012).

Morphological and ultrastructural comparison between *C. chilense* and *C. caldarium*

Light microscopy of biofilm samples revealed the presence of taxa belonging to Bacteria, Cyanobacteria, Chlorophyta, and Rhodophyta; in all samples *C. chilense* was dominant. The vegetative cells of *C. chilense* were comparable in shape and size with those already reported by Schwabe (1936), Azúa-Bustos *et al.* (2009) and Del Rosal *et al.* (2015), from European and Extra-European caves: cells ranged between

2 and 5.5 μm in diameter and were spherical or slightly elliptic in shape and exhibited a thick cell wall characterized by a smooth or gently corrugated surface (Fig. 3a,c). Transmission electron microscopy of vegetative cells of *C. chilense* and *C. caldarium* clearly showed the typical ultrastructural elements previously described by Azúa-Bustos *et al.* (2009) for *C. chilense*: a thick cell wall surrounded a protoplast and concentrically arranged thylakoid membranes containing numerous phycobilisomes; small amyloid aggregates were visible within the thylakoid membranes or, sometimes, bigger ones were present close to the center of protoplast (Fig. 3b,d,f,h). The only noteworthy ultrastructural difference between *C. chilense* from Sybil's cave and *C. caldarium* concerned the cell wall, significantly thicker in the mesophilic (180–200 nm) than in the thermoacidophilic strain (60 nm). The reproduction was asexual and the autospores (meanly 1.7–2–3 μm in diameter) were released by rupture of the maternal cell wall in both *Cyanidium* species (Fig. 3c,d,e,g). Cells in asexual reproductive stage observed by TEM showed four autospores tetrahedrally arranged inside the maternal membrane (Fig. 3d,h) separated by a characteristic Y-shaped septum, which is a typical feature of the type species of the genus *C. caldarium* also visible externally by SEM.

Analysis of the microbial components of the biofilms

The identification of the microbial components of the biofilms was achieved using DGGE as molecular technique and the species identified are listed in Table 1. Data evidenced the presence of a community made of heterotrophic and autotrophic microorganisms. The profiles revealed a total of nine species that were assigned to Bacteria (three species) Cyanobacteria (two species), Rhodophyta (one species), and Chlorophyta (three species) (Table 1). The most represented species were *Bacillus mycoides* and *C. chilense* (occurring in all the sampling points), followed by *Gloeocapsa* sp., and *Streptomyces* sp. (three sampling points) (Table 1).

Sample points III–V evidenced higher biodiversity, with communities also composed by different autotrophic microorganisms, ranging from Cyanobacteria, as *Gloeocapsa* sp. and *Chroococcidiopsis* sp., to Chlorophyta, namely *Bracteacoccus minor*, *Chlorella vulgaris* and *Scotiellopsis terrestris* (Table 1). The film of sampling point III was almost exclusively formed by *C. chilense* and bacteria (Fig. 4c,h), whereas in the other four points the presence of a multispecies consortium, albeit limited to a restricted number of microorganisms, was evident. In point IV (Fig. 4d,i) scattered colonies of coccoid Cyanobacteria, possibly *Chroococcidiopsis* sp. and *Gloeocapsa* sp. formed an upper layer, followed by a middle layer with densely packed cells of *C. chilense*, and a lower layer with numerous filaments in contact with the substrate. The points I and V showed the same film structure, made up of a thin, superficial *C. chilense* population followed by a deeper layer of heterotrophic microorganisms, with some filaments that irregularly penetrate the algal layer (Fig. 4a,b,f,g). The film sampled in point II showed a different pattern: a basal layer of heterotrophic components of the community was followed by an intermingled population of coccoid cyanobacteria and *C. chilense* cells, that were stratified on multiple layers

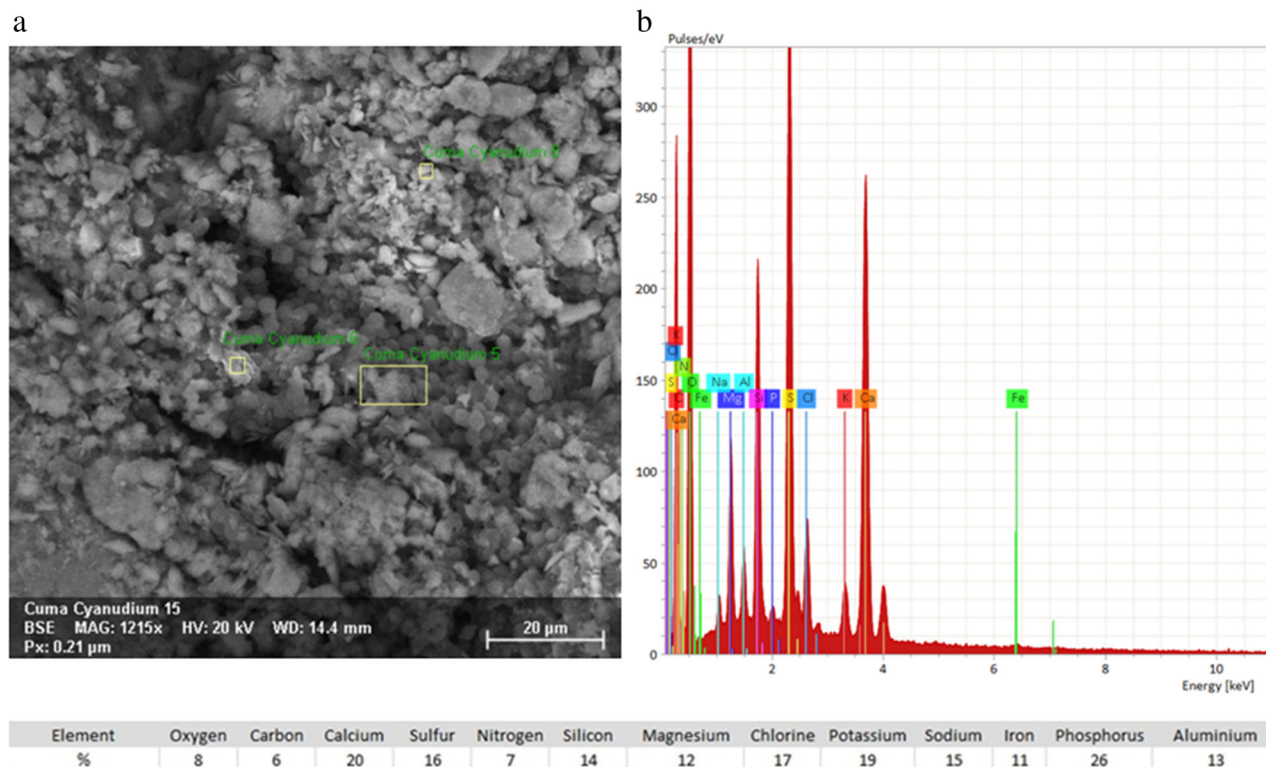


Fig. 2. Microanalysis of compared sites performed on rock substrates from which the samples were taken. (a) Scanning electron microscopy of one of the sampling sites. (b) X-ray diffractometry spectrum of the sampling site illustrated in (a).

(Fig. 4e,j). Apparently, all the other organisms detected on the basis of sequence content by DGGE were present in scarce amounts and gave a not relevant contribution to microbial films in all the sampling sites. Figure 4k–o shows the vertical distributions of the main components of sampled biofilms. As can be seen, in sampling points I, II and V, a normal distribution of *C. chilense* biomass (red line, Fig. 4k,l,o) was observed, with the heterotroph biomass (blue line) uniformly distributed along the vertical regions of the biofilm (Fig. 4k,l,o). On the other hand, the autotrophic components of the community in points III and IV (*C. chilense* and Cyanobacteria) show a plateau-shaped vertical distribution (Fig. 4m, n), whereas the peak biomass of the heterotrophic components occurred in the deepest layers of the biofilms (Fig. 4m, n). The EPS in the confocal slices showed similar patterns of vertical distribution, with a maximum prevalently located near the lithic substratum (Fig. 4k–o).

The structure of the *C. chilense* community in the five sampling points presented different features: the biofilms showed substratum coverages ranging from a minimum of 19.17% (sample point II) to a maximum of 48.64% (sample point IV). Biofilms in points I–IV were on average approximately 15 µm thick, whereas in point V the value of mean thickness was about double. In this last point was also recorded the maximum thickness, corresponding to 61.68 µm. *C. chilense* population accounted for the most part of the biofilm. EPS gave a relevant contribution to biofilm structure, except in point II (< 6%) (Table 2).

DISCUSSION

C. chilense is a unicellular rhodophyte belonging to the subphylum of Cyanidiophyceae, grouping mainly polyextremophilic microalgae all sharing the ability to thrive in hydrothermal systems, at temperatures up to 55°C and pH 0.0–5.5. Diversely from these thermo-acidophilic strains, *C. chilense* is considered as a mesophilic and neutrophilic alga, which colonizes in extreme environments such as those of caves. Our main interest was to verify the similarities/differences observed within the populations of *C. chilense* from Sybil's cave and those collected worldwide, in order to clearly describe this clade. Finally, we defined specific traits of *C. chilense* to enlighten the eco-physiological and morphological distinction from *C. caldarium*. Interestingly, this distinction is also evident on phylogenetic bases and strongly supports the hypothesis of a new algal genus within Cyanidiophyceae.

Biofilms containing *C. chilense* were collected in a site not very exposed to light and the preference for this kind of environment is widely confirmed in the literature for *C. chilense*. According to Cennamo *et al.* (2012, 2015), the mean amount of photosynthetically active radiation in Sybil's cave ranged from 0.0165 to 3.31 µE s⁻¹m⁻² and *C. chilense* was detected only in sampling sites with low to medium light intensities. Accordingly, Azúa-Bustos and Vicuña (2010) reported that the areas of the Atacama coastal cave where the biofilm mostly develops were those subjected to extremely low light intensities, as well as in the Spanish caves from Malaga (Del Rosal *et al.* 2015).

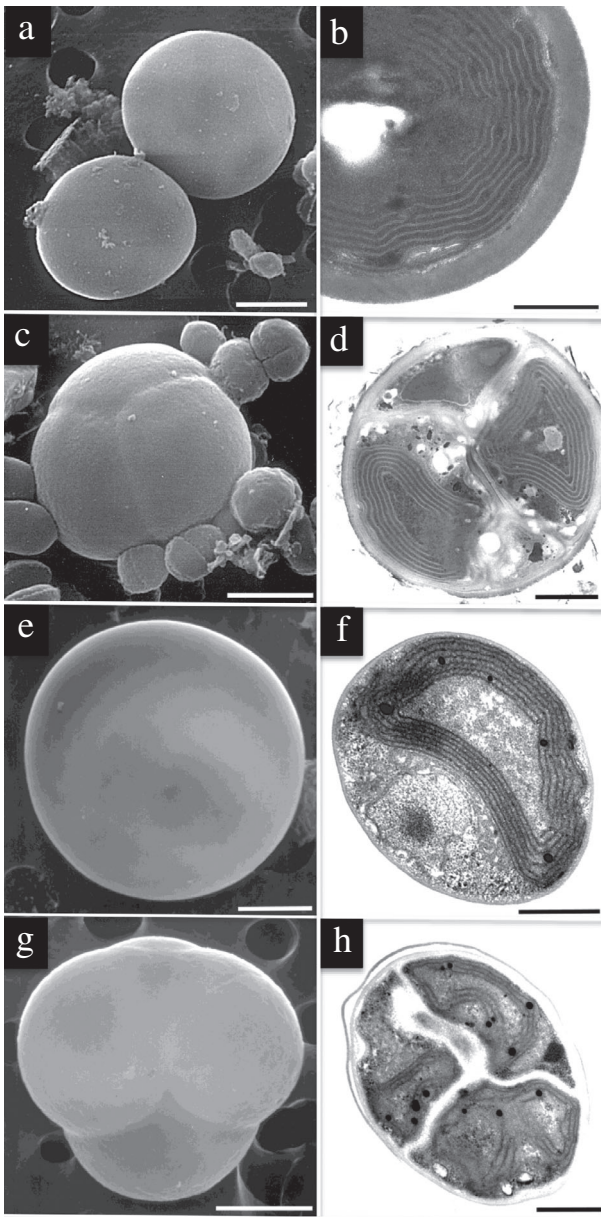


Fig. 3. Scanning and transmission electron microscopic images of *C. chilense* and *C. caldarium*. (a–d), *C. chilense*: (a) young cells, (b) cell wall, (c, d) sporangium, with typical Y-septum, (e–h) *C. caldarium*: (e, f) adult cell, (g) growing sporangium, (h) spores tetrad, scale bars: a = 1 μ m; b = 200 nm; c = 1 μ m; d = 300 nm; e = 500 nm; f = 300 nm; g = 1 μ m; h = 500 nm.

In all the selected sampling points within Sybil's cave, biofilms were primarily composed by *C. chilense*; the composition of the film-building organisms differed somehow in the investigated points, and include few photosynthetic and non-photosynthetic taxa, typically growing in cave habitats. A recent molecular characterization of the algal flora from different sites within Sybil's cave revealed a high biodiversity, since at least 20 algal species were identified, mainly represented by Cyanobacteria (11 species), followed by Chlorophyta (six), Rhodophyta (two) and Bacillariophyta (two), with a distribution dependent on humidity

and light intensity (Cennamo *et al.* 2012, 2013). A more complex algal flora in association with *C. chilense* was detected in the Neria cave, despite the species number being lower compared to that of other caves (Urzi & De Leo 2001; Albertano 2003; Roldán & Hernández-Maríné 2009). Contrarily, monospecific populations of *C. chilense* were detected in the caves at Angles (France, Leclerc *et al.* 1983) and in the coastal cave of the hyperarid Atacama desert (Azúa-Bustos *et al.* 2009); in the latter, 16S rRNA analysis carried out on the *C. chilense* biofilms excluded the presence of photosynthetic microorganisms, while only heterotrophic bacteria related to the genera *Salinispora* and *Saccharomonospora* were detected. Presumably, the constantly dry conditions and extremely low photon flux levels were incompatible with the survival of most photosynthetic organisms. According to Gladis-Schmacka *et al.* (2014), the frequency and not the amount of total water allow the proliferation of the biofilm; the variation in species composition is strongly related to the fluctuations of relative humidity along the year: dryness favored species belonging to the genus *Chroococidiopsis*, that survive in extreme conditions, being able to enter in a dormancy state with desiccation, while rehydration through air humidity induces the proliferation of the photosynthetic algal flora.

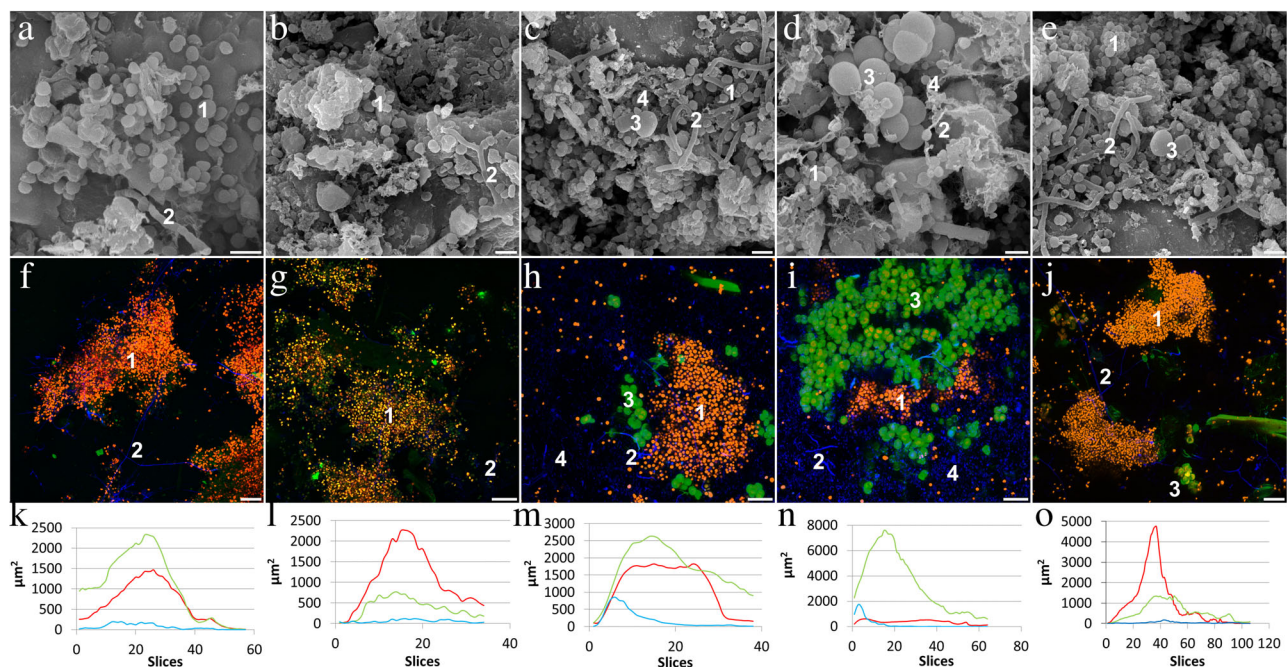
The community observed in four sampling points showed similar three-dimensional arrangements, with the heterotrophic components representing the bottom of the biofilm, in strict contact with the lithic substrate and the *Cyanidium* population scattered over higher layers. Only in sample point IV, *C. chilense* was found to be loosely surrounded by cyanobacterial cells. The structure of the biofilm suggests that the heterotrophic microorganisms are mainly involved in the attachment of the biofilm to the substrate. Over these layers *C. chilense* forms large, compact islets separated by voids. Autotrophic and heterotrophic components of *C. chilense* biofilm are stabilized by EPS, that are present in all the samples collected in the site, even though only in one sampling point we observed a reduced production of extracellular materials. EPS usually include polysaccharides, proteins, nucleic acids, and lipids; they are crucial for the mechanical stability of biofilms, mediating their adhesion to surfaces and forming a cohesive, three-dimensional polymer network interconnecting biofilm cells. EPS matrices are generally secreted to allow water retention mainly in arid and hyperarid habitats, such as deserts (Gorbushina 2007). Along with this, EPS secretion is also under quorum-sensing control which enables microorganisms to switch on and off the production of EPS, revealing microbial flexibility and regulating their metabolic machinery depending on the environmental variations and circumstances (Nadell *et al.* 2008). EPS production is a metabolically expensive energetic investment for the cells; according to Nadell *et al.* 2008, EPS activation would occur when cells reach a high cell density and would allow strains to push their lineages into nutrient-rich areas and suffocate neighboring cells, in order to sustain competition among strains; the deactivation of EPS production would occur as a metabolic strategy both to re-direct resources into growth and cell division and to allow dispersal of the algal cells.

C. chilense and *C. caldarium*

Within the biofilms sampled in Cuma, *C. chilense* vegetative cells appeared comparable in shape and size with those

Table 1. List of taxa at sampling sites in Sybil's cave, as resulted by DGGE analyses (+ presence; – absence). Occurrences are separately reported for Bacteria, Cyanobacteria, and algae in the sampling sites (I–V)

Species	GenBank codes and identities	Sampling sites					
		I	II	III	IV	V	
Bacteria	<i>Bacillus mycoides</i>	KM983002 98%	+	+	+	+	+
	<i>Bacillus megaterium</i>	DQ408589 96%	–	–	+	+	–
	<i>Streptomyces</i> sp.	D63866 99%	+	+	–	–	+
Cyanobacteria	<i>Gloeocapsa</i> sp.	JQ003611 96%	–	–	+	+	+
	<i>Chroococciopsis</i> sp.	AY790848 97%	–	–	–	–	+
Chlorophyta	<i>Bracteacoccus minor</i>	KF673367 98%	–	–	+	–	–
	<i>Chlorella vulgaris</i>	FJ864684 100%	–	–	–	+	–
	<i>Scotiellopsis terrestris</i>	AB012847 99%	–	–	–	–	+
Rhodophyta	<i>Cyanidium chilense</i>	AY391360 100%	+	+	+	+	+

**Fig. 4.** SEM (1st line) and CLSM (2nd line) images of biofilms from Sibyl's cave, Cuma, in sampling point I (a, f, k), II (b, g, l), III (c, h, m), IV (d, i, n), V (e, j, o). *C. chilense* (1), fungal hyphae (2), *Gloeocapsa* sp. (3), bacteria cells (4). In (a–e) scale bar 2 μm , in (f–j) scale bar 20 μm . Vertical profiles (k–o) of biofilm (f–j) coverage analyzed, are shown for representative samples. The red channel and red line show chlorophyll *a* autofluorescence, the blue channel and blue line represent bacteria and hyphae stained with Calcofluor-white, the green channel and green line represent EPS labeled with ConA.

already reported by Schwabe (1936), Azúa-Bustos *et al.* (2009), and Del Rosal *et al.* (2015), from European and extra-European caves, under both light microscopy and TEM. Moreover, *C. chilense* cells in the asexual reproductive stage showed the typical features previously reported for this species (Hoffmann 1994) visible by TEM or SEM.

The morphological and ultrastructural observations carried out in the present paper confirmed the similarities between *C. chilense* and *C. caldarium* already detected in previous papers; the main diacritic features, such as the plastid morphology, the arrangement of the thylakoids, the vegetative reproduction and the production of four autospores

Table 2. Analysis of the selected parameters of sampled biofilms

Sampling point	Substratum coverage MIP(%)	Biomass (μm^3)	Th mean (μm)	Th max (μm)	Autotrophic <i>C. chilense</i> (%)	AutotrophicOther species (%)	Heterotrophic (%)	EPS (%)	Source
I	28.16	54 065.14	16.89	39.84	35.52	0.06	7.54	56.88	Present paper
II	19.17	31 790.89	12.78	23.54	64.36	1.87	27.94	5.83	Present paper
III	24.09	56 147.26	15.16	21.73	33.44	2.93	10.36	53.27	Present paper
IV	48.64	146 730.9	15.55	37.01	7.40	1.80	6.14	84.66	Present paper
V	24.51	78 532.89	32.44	61.68	58.88	1.86	3.80	35.46	Present paper
	—	—	—	—	P	A	A	P	Azúa-Bustos <i>et al.</i> 2009
	—	—	—	—	P	4 taxa	A	A	Cennamo <i>et al.</i> 2012
	—	—	—	—	P	1 taxa	A	A	Del Rosal <i>et al.</i> 2015
	—	—	—	—	P	—	—	—	Darienko & Hoffmann 2010
	—	—	—	—	P	—	—	—	Friedmann 1964
	—	—	—	—	P	—	—	—	Gaylarde <i>et al.</i> 2012
	—	—	—	—	P	—	—	—	Leclerc <i>et al.</i> 1983
	—	—	—	—	P	—	—	—	Skuja 1970

A, absent; P, present; Th, thickness.

were shared by both species. Despite the lack of diagnostic characters helpful to discriminate between the mesophilic and the thermophilic *Cyanidium*, it is noteworthy that all *C. chilense* strains share three fundamental aspects related to the necessity to withstand desiccation and water fluctuations, and maintain the integrity of cellular organelles: (i) the thickening of the cell wall; in *C. chilense* from Sybil's cave it ranged from 180 to 390 nm, while *C. caldarium* from our cultures showed a thin wall around the cells, 60 nm approximately; this trait was also visible from TEM micrographs in *C. chilense* from Atacama desert and from the Spanish cave, as well as in the electron micrographs of the mesophilic strains identified by Hoffmann from the cave at Angles (France); (ii) the strict association among the cells, forming multilayered islets on the top soil or even within the upper millimeters of the soil; this strategy again would contribute to reducing water loss better than when cells are solitarily living; (iii) the production of EPS, never observed in environmental samples of *C. caldarium*, but common to all *C. chilense* to date analyzed.

CONCLUSIONS

Taken together, all the data collected from this and previous studies have allowed a better delineation of the ecophysiological and morphological traits of *C. chilense*. The morphophysiological diagnosis, the monophyly of the mesophilic *C. chilense* strains, clustering separately from the

thermoacidophilic *C. caldarium*, along with the deeper genomic investigation, strongly support the institution of a new algal genus within Cyanidiophyceae.

REFERENCES

- Albertano, P. 2003. Methodological approaches to the study of stone alteration caused by cyanobacterial biofilms in hypogean environments. In Koestler, R. J., Koestler, V. R., Charola, A. E. and Nieto-Fernandez, F. E. (Eds). *Art, Biology, and Conservation: Biodeterioration of Works of Art*. The Metropolitan Museum of Art, New York, pp. 302–15.
- Azúa-Bustos, A., González-Silva, C., Mancilla, R. A. *et al.* 2009. Ancient photosynthetic eukaryote biofilms in an Atacama Desert coastal cave. *Microb. Ecol.* **58**: 485–96.
- Azúa-Bustos, A. and Vicuña, R. 2010. Chilean cave *Cyanidium*. In Seckbach, J. and Chapman, D. J. (Eds). *Red Algae in Genomic Age. Cellular Origin, Life in Extreme Habitats and Astrobiology, Vol. 13*. Springer, Dordrecht, pp. 429–39.
- Baveye, P. 2002. Comment on evaluation of biofilm image thresholding methods. *Water Res.* **36**: 805–6.
- Brock, T. D. 1978. The genus *Cyanidium*. In Starr, P. M. (Ed.). *Thermophilic Microorganisms and Life at High Temperatures*. Springer-Verlag, New York, pp. 255–301.
- Carfagna, S., Landi, V., Coraggio, F. *et al.* 2018. Different characteristics of C-phycocyanin (C-PC) in two strains of the extremophilic *Galdieria phlegrea*. *Algal Res.* **31**: 406–12.
- Castenholz, R. W. 2001. Phylum Bx. Cyanobacteria. In Boone, D. R., Castenholz, R. W. and Garrity, G. M. (Eds). *Bergey's Manual of Systematic Bacteriology*, Springer, New York, NY, pp. 473–599.

- Cennamo, P., Caputo, P., Giorgio, A., Moretti, A. and Pasquino, N. 2013. Biofilms on tuff stones of cultural heritage: identification and removal by non-thermal effects of radiofrequencies. *Microb. Ecol.* **66**: 659–68.
- Cennamo, P., Caputo, P., Marzano, C., Miller, A. Z., Saiz-Jimenez, C. and Moretti, A. 2015. Diversity of phototrophic components in biofilms from Piperno historical stoneworks. *Plant Biosyst.* **150**: 720–9.
- Cennamo, P., Marzano, C., Ciniglia, C. *et al.* 2012. A survey of the algal flora of anthropogenic caves of Phlegrean Fields (Naples, Italy) archeological district. *J. Cave Karst Stud.* **74**: 243–50.
- Cennamo, P., Montuori, N., Trojsi, G., Fatigati, G. and Moretti, A. 2016. Biofilms in churches built in grottoes. *Sci. Total Environ.* **543**: 727–38.
- Ciniglia, C., Mastrobuoni, F., Scortichini, M., Petriccione, M. 2015. Oxidative damage and cell-programmed death induced in *Zea mays* L. by allelochemical stress. *Ecotoxicology* **24**(4): 926–937.
- Ciniglia, C., Pinto, G. and Pollio, A. 2018. *Cyanidium* from caves: a reinstatement of *Cyanidium chilense* Schwabe (Cyanidiophytina, Rhodophyta). *Phytotaxa* **295**: 86–88.
- Ciniglia, C., Yang, E. C., Pollio, A. *et al.* 2014. Cyanidiophyceae in Iceland: plastid *rbcL* gene elucidates origin and dispersal of extremophilic *Galdieria sulphuraria* and *G. maxima* (Galdieriaceae, Rhodophyta). *Phycologia* **53**: 542–51.
- Ciniglia, C., Yoon, H. S., Pollio, A., Pinto, G. and Bhattacharya, D. 2004. Hidden biodiversity of the extremophilic Cyanidiales red algae. *Mol. Ecol.* **13**: 1827–38.
- Darienko, T. and Hoffmann, L. 2010. Subaerial algae and cyanobacteria from the archaeological remains of Carthage (Tunisia), including the record of a species of *Cyanidium* (Rhodophyta). *Algol. Stud.* **135**: 41–60.
- Del Mondo, A., Pinto, G., Carbone, D. A., Pollio, A. and De Natale, A. 2018. Biofilm architecture on different substrates of an *Oculatella* subterranea (Cyanobacteria) strain isolated from Pompeii archaeological site (Italy). *Environ. Sci. Pollut. Res.* **25** (26): 26079–89.
- Del Rosal, Y., Jurado, V., Roldán, M., Hernández Mariné, M. and Sáiz-Jiménez, C. 2015. *Cyanidium* sp. colonizadora de cuevas turísticas. In Oliva, M. Moreno, Rogerio-Candelera, M. A., López Navarrete, J. T. and Jolín, V. H. (Eds). *Estudio y Conservación del Patrimonio Cultural*. Actas, Universidad de Málaga, Malaga, pp. 170–3.
- Di Girolamo, P., Ghiara, M. R., Lirer, L., Munno, R., Rolandi, G. and Stanzione, D. 1984. Vulcanologia e petrografia dei Campi Flegrei. *Bull. Geol. Soc. It.* **103**: 349–413.
- Diez, B., Pedros-Alio, C., Marsh, T. L. and Massana, R. 2001. Application of denaturing gradient gel electrophoresis (DGGE) to study the diversity of marine picoeukaryotic assemblages and comparison of DGGE with other molecular techniques. *Appl. Environ. Microbiol.* **67**: 2942–51.
- Doyle, J. J. and Doyle, J. L. 1990. A rapid DNA isolation procedure for small quantities of fresh leaf tissue. *Phytochem. Bull.* **19**: 11–5.
- Eren, A., Iovinella, M., Yoon, H. S. *et al.* 2018. Genetic structure of *Galdieria* populations from Iceland. *Polar Biol.* **41**: 1681–91.
- Friedmann, I. 1964. Progress in the biological exploration of caves and subterranean waters in Israel. *Int. J. Speleol.* **1** (1): 29–33.
- Gaylarde, C. C., Gaylarde, P. M. and Neilan, B. A. 2012. Endolithic phototrophs in built and natural stone. *Curr. Microbiol.* **65**: 183–8.
- Gaylarde, P. M., Jungblut, A. D., Gaylarde, C. C. and Neilan, B. A. 2006. Endolithic phototrophs from an active geothermal region in New Zealand. *Geomicrobiol. J.* **23** (7): 579–87.
- Gladis-Schmacka, F., Glatzel, S., Karsten, U., Bottcher, H. and Schumann, R. 2014. Influence of local climate and climate change on aeroterrestrial phototrophic biofilms. *Biofouling* **30** (4): 401–14.
- Gorbushina, A. A. 2007. Life on the rocks. *Environ. Microbiol.* **9** (7): 1613–31.
- Hartig, S. M. 2013. Basic image analysis and manipulation in ImageJ. *Curr. Protoc. Mol. Biol.* **102**(1):14.15.1–14.15.12.
- Heydorn, A., Ersbøll, B. K., Hentzer, M., Parsek, M. R., Givskov, M. and Molin, S. 2000. Quantification of biofilm structures by the novel computer program comstat. *Microbiol-ogy* **146**: 2395–407.
- Hoffmann, L. 1994. *Cyanidium*-like algae from caves. In Seckbach, J. (Ed.). *Evolutionary Pathways and Enigmatic Algae: Cyanidium Caldarium (Rhodophyta) and Related Cells*, pp. 175–82. Springer, Berlin, Germany.
- Holzinger, A. and Lütz, C. 2006. Algae and UV irradiation: effects on ultrastructure and related metabolic functions. *Micron* **37**: 190–207.
- Iovinella, M., Eren, A., Pinto, G. *et al.* 2018. Cryptic dispersal of Cyanidiophytina (Rhodophyta) in non-acidic environments from Turkey. *Extremophiles* **22** (5): 713–23.
- Leclerc, J. C., Couté, A. and Dupuy, P. 1983. Le climat annuel de deux grottes et d'une église du Poitou, ou vivent des colonies pures d'algues sciaphiles. *Cryptogamie Algol.* **4** (1–2): 1–19.
- Lepanto, P., Lecumberry, F., Rossello, J. and Kierbel, A. 2014. A confocal microscopy image analysis method to measure adhesion and internalization of *Pseudomonas aeruginosa* multicellular structures into epithelial cells. *Mol. Cell. Probes* **28** (1): 1–5.
- Marasco, D., Nocerino, S., Pinto, G., Pollio, A., Troisi, G. and De Natale, A. 2016. Weathering of a Roman mosaic – a biological and quantitative study on in vitro colonization of calcareous tesserae by phototrophic microorganisms. *PLoS One* **11** (10): e0164487.
- Nadell, C. D., Xavier, J. B., Levin, S. A. and Foster, K. R. 2008. The evolution of quorum sensing in bacterial biofilms. *PLoS Biol.* **6** (1): e14.
- Pedersen, K. 2000. Exploration of deep intraterrestrial microbial life: current perspectives. *FEMS Microbiol. Lett.* **185** (1): 9–16.
- Roldán, M. and Hernández-Mariné, M. 2009. Exploring the secrets of the three-dimensional architecture of phototrophic biofilms in caves. *Int. J. Speleol.* **38**: 41–53.
- Schindelin, J., Arganda-Carreras, I., Frise, E. *et al.* 2012. Fiji: an open-source platform for biological-image analysis. *Nat. Methods* **9** (7): 676–82.
- Schwabe, G. H. 1936. *Über Einige Blaualgen aus dem Mittleren und Südlichen Chile*. Deutscher Wissenschaftlicher Verein Santiago, Santiago de Chile, Chile.
- Schwabe, G.H. 1942. Über das Thermalbad Kusatu. Mitteilungen Der Deutschen. Gesellschaft for Natur- und Völklerkunde Ostasiens. Otto Harrassowitz, Tokyo, Leipzig, Band XXIII (Teil C), pp. C41–C42.
- Skuja, H. 1970. Alghe cavernicole nelle zone illuminate delle Grotte di Castellana (Murge di Bari). *Le Grotte d'Ital.* **4**: 193–202.
- Solé, A., Diestra, E. and Esteve, I. 2009. Confocal laser scanning microscopy image analysis for cyanobacterial biomass determined at microscale level in different microbial mats. *Microb. Ecol.* **57**: 649–56.
- Urzi, C. and De Leo, F. 2001. Sampling with adhesive tape strips: an easy and rapid method to monitor microbial colonization on monument surfaces. *J. Microbiol. Methods* **44**: 1–11.
- Yoon, H. S., Müller, K. M., Sheath, R. G., Ott, F. D. and Bhattacharya, D. 2006. Defining the major lineages of red algae (Rhodophyta). *J. Phycol.* **42** (2): 482–92.